

Electronic Supporting Information

Boolean-Chemotaxis of Logibots Deciphering the Motions of Self-Propelling Microorganisms

Tamanna Bhuyan,^a Mitradip Bhattacharjee,^a Amit Kumar Singh,^a Siddhartha Sankar
Ghosh,^{a,b*} and Dipankar Bandyopadhyay^{a,c*}

^a*Centre for Nanotechnology, Indian Institute of Technology Guwahati, Assam - 781039, India.*

^b*Department of Biosciences and Bioengineering, Indian Institute of Technology Guwahati,
Assam-781039, India.*

^c*Department of Chemical Engineering, Indian Institute of Technology Guwahati, Assam -
781039, India.*

*Corresponding Authors: sghosh@iitg.ernet.in, dipban@iitg.ernet.in

1. Characterization of logibots

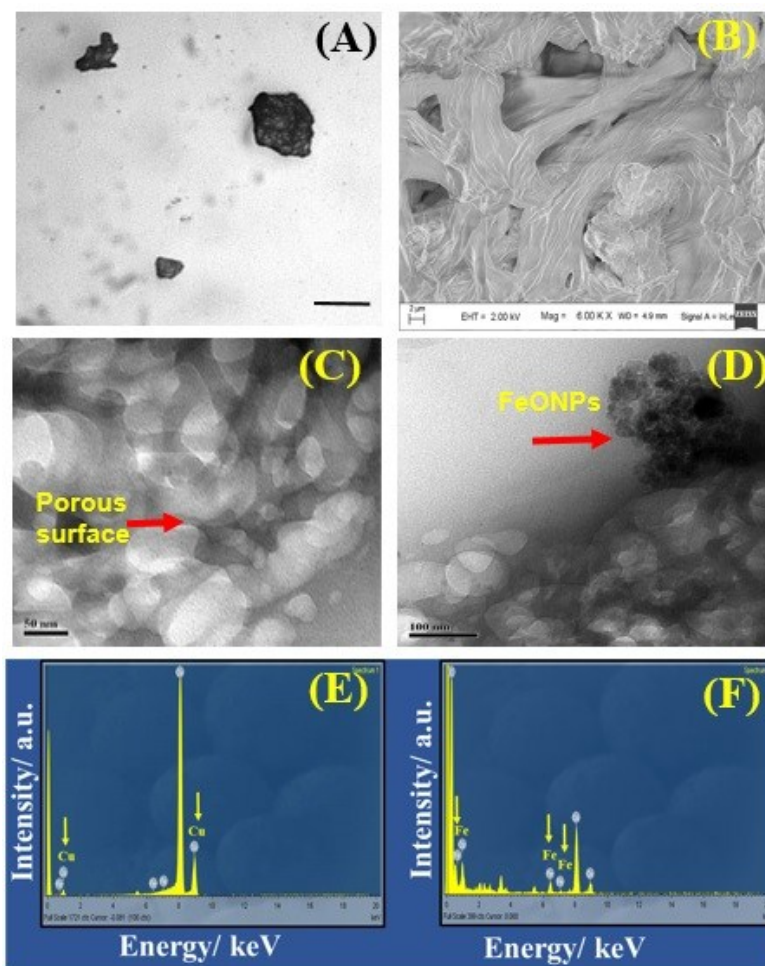


Figure S1. Image (A) shows the optical micrograph of logibots observed under the Leica DM 2500 upright microscope, where the scale bar is 200 μm . Image (B) shows the Field emission scanning electron microscopy (FESEM) image of the logibot's surface. The scale bar at the bottom is of 2 μm . Transmission electron microscopy (TEM) image (C) shows a logibot displaying porous morphology. The scale bar is of 50 nm. Image (D) shows a logibot having the magnetite nanoparticles (FeONPs) deposited on the surface where the scale bar is of 100 nm. Energy Dispersive X-ray (EDX) spectra in the image (E) corresponds to the uncoated logibots. The EDX plot in the image (F) shows the presence of the FeONPs on the logibot, indicated by the downward yellow arrows.

The optical micrograph of the logibot is shown in **Figure S1A** with size ranging from $\sim 50 - 150$ μm . The surface morphology of logibot is shown by the FESEM image in the **Figure S1B**. The surface porosity of the logibot is displayed in TEM micrograph, **Figure S1C**. The deposition of

aggregates of magnetite nanoparticles (FeONPs) on the motor surface was observed in the TEM micrograph **Figure S1D**. The surface of uncoated micromotor displayed the presence of Cu from the TEM grid and small amount of inherent iron (Fe) in the uncoated logibot, as shown in EDX plot in the **Figure S1E**. The EDX of FeONPs-coated logibot in **Figure S1F** shows the presence of elemental Fe (0.72%), indicated by the downward yellow arrows. The above figures confirmed the coating of FeONPs aggregates on the porous surface of logibots.

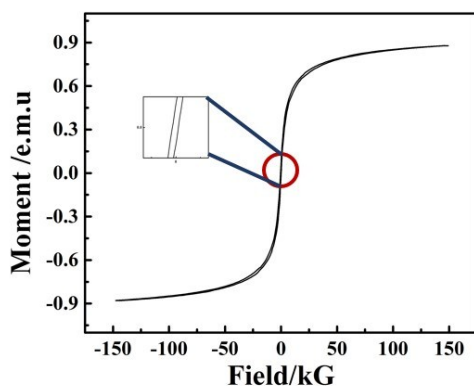


Figure S2. Image shows the vibrating sample magnetometry (VSM) of the logibots.

The magnetization saturation of the logibots were measured by the VSM analysis at 25°C when the magnetic field strength was varied from -15 to 15 kG. The magnetization curve of the logibots shown in **Figure S2** has the M_s value of $\sim 0.594 \text{ emu g}^{-1}$. The curve confirms the deposition of FeONP aggregates on the surface of logibot.

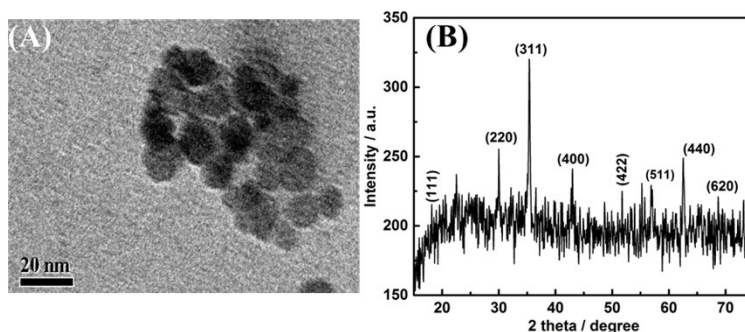


Figure S3. (A) TEM image of magnetite nanoparticles (FeONPs). (B) XRD analysis of FeONPs. The scale bar at the bottom is 20 nm.

The TEM micrographs of FeONPs in **Figure S3A** revealed that they exhibited spherical shape with a narrow size distribution of $\sim 7 - 5$ nm. The XRD pattern in **Figure S3B** showed consistent and broad diffraction peaks at $2\theta = 18.55^\circ, 30.1^\circ, 35.5^\circ, 43.15^\circ, 53.45^\circ, 57.6^\circ, 62.6^\circ,$ and 68.88° corresponding to the (111), (220), (311), (400), (422), (511), (440), and (620) crystallographic planes of FeONPs with the standard pattern of JCPDS CARD No.19-0629.¹⁻⁵

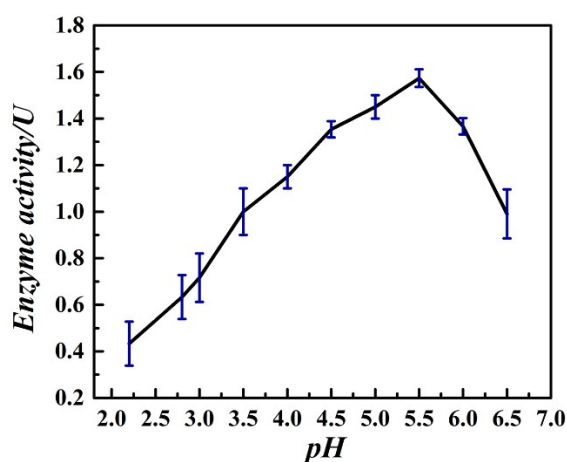


Figure S4. Image shows catalase activity of logibots under a varying pH range.

The activity of inherent catalase enzyme in the micromotors and catalase-HCl drip solutions were estimated by using a method reported previously.¹ The samples were prepared using the reported method and evaluated in triplicates for each samples by measuring the absorbance of catalase (A_{240}) using a TECAN microplate reader. The catalase activity of the logibots was evaluated considering a varying pH window of 2.5 to 6.0. The optimum pH range for maximal activity of catalase was found to be between 2.8 to 5.5, beyond which the activity was diminished. A gradual decrease in enzyme activity could be observed with $\text{pH} < 2.8$ and $\text{pH} > 5.5$, i.e., ~ 0.4 U and which and ~ 1.7 U, respectively. The enzyme activity is usually affected by pH changes beyond its

favorable range.⁶ Since pH is one of the factors responsible in protein denaturation, the exposure to enzyme catalase in highly acidic and basic pH solutions could destroy the secondary and tertiary structure of enzyme leading to gross reduction in the enzymatic activity.⁷

2. Experimental details of logibot migration

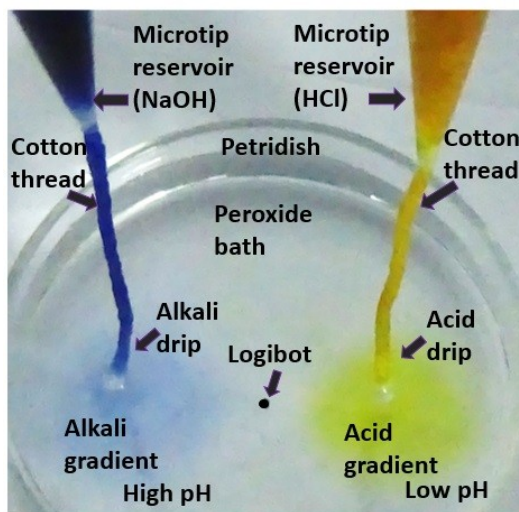


Figure S5. Schematic diagram of the experimental set-up to study the motions of a logibot.

The **Figure S5** shows setup employed to perform the self-propelling motions of the logibots.¹ Dual micropipette tips were used as chemical reservoirs containing alkali and acid inputs in a petridish (3 cm diameter) containing 6 mL of 7.0% (v/v) H_2O_2 fuel. The acid (HCl) gradient was introduced ~ 3 mm away from the center of the petridish with the help of a cotton thread connected to a chamber containing a uniform solution of 0.005 M HCl and 2 ppm of catalase. The alkali (0.3 M NaOH) gradient was established at ~ 11 mm away from the acid gradient by using a cotton thread connected to a reservoir. The thymol blue indicator (0.2 g in 50 mL) was dispensed on the peroxide bath to point out the pH gradient. The logibot (dia. ~ 140 μm) was introduced nearly at the midpoint of the two threads. In order to nullify the thread effect, the motor speed was calculated by

measuring the displacement of the motor from an initial point to a position of ~ 6.5 mm away from the thread. The experiments were carried out thrice for each pH value and the velocity of the motor was studied at different pH values of the chemical drip.

3. Supporting Videos

Supporting video S1: The video shows the chemotactic migration of a logibot (~ 140 μm) under the influence of an alkali gradient. The motor migrated towards the alkali pH gradient when it was suspended in a petridish of 7% (v/v) peroxide fuel with an alkali rich zone (blue). The alkali gradient was introduced by continuous dripping of 0.3 M NaOH solution that was tracked by thymol blue indicator which presented blue coloration in the alkaline region.

Supporting video S2: The video shows the repulsive migration of a logibot (~ 140 μm) in 7.0% (v/v) peroxide bath under the influence of continuous 0.005 M HCl drips. The motor repelled away from the acidic source. The acid gradient was tracked by thymol blue indicator, which presented yellow coloration in the region of gradient.

Supporting video S3: The video shows the chemotactic migration of a logibot (~ 140 μm) in 7.0% (v/v) peroxide bath under the influence of continuous catalase-HCl drips. The acid gradient was tracked by thymol blue indicator, which presented yellow coloration in the region of gradient. The motor migrated towards the acidic gradient (region of low pH).

Supporting video S4: The video shows the motion of the logibot (~ 150 μm) towards the HCl-catalase drip (pH ~ 4.51) in dual acid-alkali gradient system. The advancing alkali and acid front in all the experiments were observed using thymol blue indicator in the peroxide bath.

Supporting video S5: The video shows the motion of the logibot away the HCl-catalase drip (pH ~ 2.46) but towards the NaOH drip in dual acid-alkali gradient system. The advancing alkali and acid front in all the experiments were observed using thymol blue indicator in the peroxide bath.

Supporting video S6: The video shows the stationary state of logibot (~ 140 μm) in 7.0% (v/v) peroxide bath. The motor showed no motion in the bath due to isotropic generation of oxygen bubbles from the all different directions of the surface of logibot.

References

1. T. Bhuyan, A. K. Singh, D. Dutta, A. Unal, S. S. Ghosh and D. Bandyopadhyay, *ACS Biomater. Sci. Eng.*, 2017, **3**, 1627-1640.
2. S. Aliramaji, A. Zamanian and Z. Sohrabijam, *Procedia Mater. Sci.*, 2015, **11**, 265-269.
3. T. R. Bastami and M. H. Entezari, *Mater. Res. Bull.*, 2013, **48**, 3149-3156.
4. S. Mahadevan, S. P. Behera, G. Gnanaprakash, T. Jayakumar, J. Philip and B. P. C. Rao, *J. Phys. Chem. Solids*, 2012, **73**, 867-872.
5. Y. Wang, B. Li, Y. Zhou, and D. Jia, *Nanoscale Res. Lett.*, 2009, **4**, 1041-1046.
6. S. Morgulis, M. Beber and I. Rabkin, *J. Biol. Chem.*, 1926, **68**, 547-563.
7. S. Susmitha, P. Ranganayaki, K. K. Vidyamol and R. Vijayaraghavan, *Int. J. Curr. Microbiol. Appl. Sci.*, 2013, **2**, 255-263.